

# Neural Architecture Search for Speech Recognition

Shoukang Hu, Xurong Xie, Shansong Liu, Mengzhe Geng, Xunying Liu, Helen Meng

The Chinese University of Hong Kong, Hong Kong SAR, China

{skhu, ssliu, mzgeng, xyliu, hmmeng}@se.cuhk.edu.hk {xrxie}@ee.cuhk.edu.hk

## Abstract

Deep neural networks (DNNs) based automatic speech recognition (ASR) systems are often designed using expert knowledge and empirical evaluation. In this paper, a range of neural architecture search (NAS) techniques are used to automatically learn two hyper-parameters that heavily affect the performance and model complexity of state-of-the-art factored time delay neural network (TDNN-F) acoustic models: i) the left and right splicing context offsets; and ii) the dimensionality of the bottleneck linear projection at each hidden layer. These include the standard DARTS method fully integrating the estimation of architecture weights and TDNN parameters in lattice-free MMI (LF-MMI) training; Gumbel-Softmax DARTS that reduces the confusion between candidate architectures; Pipelined DARTS that circumvents the overfitting of architecture weights using held-out data; and Penalized DARTS that further incorporates resource constraints to adjust the trade-off between performance and system complexity. Parameter sharing among candidate architectures was also used to facilitate efficient search over up to  $7^{28}$  different TDNN systems. Experiments conducted on a 300-hour Switchboard conversational telephone speech recognition task suggest the NAS auto-configured TDNN-F systems consistently outperform the baseline LF-MMI trained TDNN-F systems using manual expert configurations. Absolute word error rate reductions up to 1.0% and relative model size reduction of 28% were obtained.

**Index Terms:** Neural Architecture Search, Time Delay Neural Network, Speech Recognition

## 1. Introduction

Deep neural networks (DNNs) play a central role in state-of-the-art automatic speech recognition (ASR) systems[1, 2, 3, 4]. When designing these systems, a set of neural network structure design decisions such as the hidden layer dimensionality and connectivity need to be made. These decisions are largely based on expert knowledge or empirical choice to date. As explicitly training and evaluating the performance of different network architectures is highly expensive, it is preferable to use automatic neural architecture design techniques.

To this end, neural architecture search (NAS) approaches [5] have gained increasing research interests in recent years. The key objectives of NAS methods are three fold. First, it is crucial to produce an accurate performance ranking over different candidate neural architectures to allow the best system to be selected. Second, when operating at the same level of accuracy performance target, preference should be given to simpler architectures with fewer parameters in order to minimize the risk of overfitting to limited data. Furthermore, to ensure scalability and efficiency on large data sets, a search space containing all candidate systems of interest needs to be defined.

Earlier forms of NAS techniques were based on neural evolution [6], where genetic algorithms were used to randomly se-

lect architecture choices at each iteration of structural mutation and crossover. Bayesian NAS methods based on Gaussian Process was proposed in [7]. Reinforcement learning (RL) based NAS approaches [8, 9, 10, 11, 12] have also been developed. In these techniques, explicit system training and evaluation are required. In addition, as the architecture hyper-parameters and actual DNN parameters are separately learned, e.g., within the RL controller and candidate systems, a tighter integration of both is preferred during NAS.

Alternatively, differentiable architectural search (DARTS) techniques can be used [13, 14, 15, 16, 17]. Architectural search is performed over an over-parameterized parent super-network containing paths connecting all candidate DNN structures to be considered. The search is transformed into the estimation of the weights assigned to each candidate neural architecture within the super-network. The optimal architecture is obtained by pruning lower weighted paths. This allows both architecture selection and candidate DNN parameters to be consistently optimized within the same super-network model.

In contrast to the rapid development of NAS techniques in the machine learning and computer vision communities, there has been very limited research of applying these to speech recognition systems so far. In this paper, a range of DARTS based NAS techniques are used to automatically learn two architecture hyper-parameters that heavily affect the performance and model complexity of state-of-the-art factored time delay neural network (TDNN-F) [18, 19, 20, 4] acoustic models: i) the left and right splicing context offsets; and ii) the dimensionality of the bottleneck linear projection at each hidden layer. These include the standard DARTS method fully integrating the estimation of architecture weights and TDNN parameters in lattice-free MMI (LF-MMI) training; Gumbel-Softmax DARTS that reduces the confusion between candidate architectures; pipelined DARTS that circumvents the overfitting of architecture weights using validation data; and penalized DARTS that further incorporates resource constraints to flexibly adjust the trade-off between performance and system complexity. Parameter sharing among candidate architectures was also used to facilitate efficient search over a large number of TDNN systems. Experiments conducted on a 300-hour Switchboard conversational telephone speech recognition task suggest the NAS configured TDNN-F systems consistently outperform the baseline LF-MMI trained TDNN-F systems using manually designed configurations. Absolute word error rate reductions up to 1.0% and model size reduction of 28% relative were obtained.

To the best of our knowledge, this paper is among the first to apply neural architecture search techniques to speech recognition tasks. In contrast, the vast majority of previous NAS research has been focused on computer vision applications [21, 22, 23, 24, 25, 26]. Existing NAS works in the speech community were limited to key word spotting tasks [27, 28].

The rest of this paper is organized as follows. Section 2 presents a set of differentiable neural architecture search tech-

niques. Section 3 discusses the search space of TDNN-F models and necessary parameter sharing to improve the search efficiency. Section 4 presents the experiments and results. Finally, the conclusions are drawn in Section 5.

## 2. Neural Architecture Search

In this section, we present various forms of differentiable neural architecture search (DARTS) methods. With no loss of generality, we introduce the general form of DARTS architecture selection methods [13, 14, 15, 17]. For example, the  $l$ -th layer output  $\mathbf{h}^l$  can be computed as follows in the DARTS supernet:

$$\mathbf{h}^l = \sum_{i=0}^{N^l-1} \lambda_i^l \phi_i^l(\mathbf{W}_i^l \mathbf{h}^{l-1}) \quad (1)$$

where  $\lambda_i^l$  is the architecture weight for the  $i$ -th candidate choice in the  $l$ -th layer,  $N^l$  is the total number of choices in this layer. The precise form of neural architectures being considered at this layer is determined by the linear transformation parameter  $\mathbf{W}_i^l$  and activation function  $\phi_i^l(\cdot)$  used by each candidate system. For example, when selecting the TDNN-F hidden layer context offsets, the linear transformation is a binary-valued matrix for each candidate architecture, and  $\phi_i^l(\cdot)$  is represented by an identity matrix. When selecting the dimensionality of the bottleneck linear projection at each hidden layer of the factored TDNN systems, the linear transformation  $\mathbf{W}_i^l = \widehat{\mathbf{W}}_i^l \widehat{\mathbf{W}}_i^{l^T}$  is a decomposed matrix, while  $\phi_i^l(\cdot)$  is also an identity matrix.

### 2.1. Softmax DARTS

Conventional DARTS [13] system uses a Softmax function to model the architecture selection weight  $\lambda_i^l$  as

$$\lambda_i^l = \frac{\exp(\log \alpha_i^l)}{\sum_{j=0}^{N^l-1} \exp(\log \alpha_j^l)} \quad (2)$$

When using the standard back-propagation algorithm to update the architecture weights parameter  $\lambda_i^l$ , the loss function (including LF-MMI criterion [4] considered in this paper) gradient against the  $\lambda_i^l$  is computed as below.

$$\frac{\partial \mathcal{L}}{\partial \log \alpha_k^l} = \frac{\partial \mathcal{L}}{\partial \mathbf{h}^l} \sum_{i=0}^{N^l-1} \left( 1_{i=k} \lambda_i^l - \lambda_i^l \lambda_k^l \right) \phi_i^l(\mathbf{W}_i^l \mathbf{h}^{l-1}) \quad (3)$$

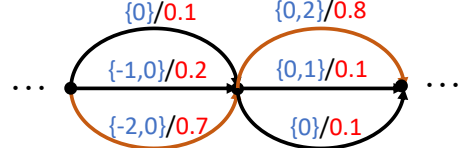
where  $1_{i=k}$  is the indicator function.

When the DARTS supernet containing both architecture weights and normal DNN parameters is trained to convergence, including architecture parameters and normal DNN parameters, the optimal architecture can be obtained by pruning lower weighted architectures that are considered less important. However, when similar architecture weights are obtained using a flattened Softmax function, the confusion among different candidate systems increases and search errors may occur.

### 2.2. Gumbel-Softmax DARTS

In order to address the above issue, a Gumbel-Softmax distribution [29] is used to sharpen the architecture weights to produce approximately a one-hot vector [14]. This allows the confusion between different architectures to be minimised. The architecture weights are computed as,

$$\lambda_i^l = \frac{\exp((\log \alpha_i^l + G_i^l)/T)}{\sum_{j=0}^{N^l-1} \exp((\log \alpha_j^l + G_j^l)/T)} \quad (4)$$



$$\begin{aligned} \{-2,0\} \{0\}: 0.7*0.1; \{-2,0\} \{0,1\}: 0.7*0.1; \{-2,0\} \{0,2\}: 0.7*0.8; \\ \{-1,0\} \{0\}: 0.2*0.1; \{-1,0\} \{0,1\}: 0.2*0.1; \{-1,0\} \{0,2\}: 0.2*0.8; \\ \{0\} \{0\}: 0.1*0.1; \{0\} \{0,1\}: 0.1*0.1; \{0\} \{0,2\}: 0.1*0.8; \end{aligned}$$

Figure 1: Part of an example NAS lattice containing architecture weights. Blue integers denote different TDNN-F context offset choices, while red integers are their associated weights. Among all 9 possible context choices shown in the figure, the brown colored path with  $+/2$  offsets is chosen with the highest probability  $0.7 * 0.8 = 0.56$ .

where  $G_i^l = -\log(-\log(U_i^l))$  is the Gumbel variable, and  $U_i^l$  is a uniform random variable. When the temperature parameter  $T$  approaches 0, it has been shown that the Gumbel-Softmax distribution is close to a categorical distribution [29].

Different samples of the uniform random variable  $U_i^l$  lead to different values of  $\lambda_i^l$  in Eq. 4. The loss function gradient w.r.t  $\log \alpha_k^l$  is computed as an average over  $J$  samples of the architecture weights as below,

$$\frac{\partial \mathcal{L}}{\partial \log \alpha_k^l} = \frac{1}{J} \sum_{j=0}^J \frac{\partial \mathcal{L}}{\partial \mathbf{h}^{l,j}} \sum_{i=0}^{N^l-1} \frac{1_{i=k} \lambda_i^{l,j} - \lambda_i^{l,j} \lambda_k^{l,j}}{T} \phi_i^l(\mathbf{W}_i^l \mathbf{h}^{l-1,j}) \quad (5)$$

where  $\lambda^{l,j}$  is the  $j$ -th sample weights vector drawn from the Gumbel-Softmax distribution in  $l$ -th layer,  $\mathbf{h}^{l,j}$  is the output of  $l$ -th layer by using the  $j$ -th sample  $\lambda^{l,j}$ . By default we assume the Gumbel-Softmax variables  $\lambda^l$  at different layers are independent among themselves.

### 2.3. Pipelined DARTS

As both architecture weights and normal DNN parameters are learned at the same time in Softmax DARTS and Gumbel-Softmax DARTS systems, the search algorithms may prematurely select sub-optimal architectures at an early stage. Inspired by [30], we decouple the update of normal DNN parameters and architecture weights into two separate stages performed in sequence. This leads to the pipelined DARTS approach. In order to prevent overfitting to the training data, a separate held-out data set taken out of the original training data is used. In Pipelined DARTS systems, the normal DNN parameters are updated to convergence on the training data first, while randomly sampled one-hot architecture weights drawn from a uniform distribution are used. In the following stage, we fix the normal DNN parameters estimated in the first stage in the supernet and update the architecture weights using the held-out data for both Softmax DARTS and Gumbel-Softmax DARTS. This produces the Pipelined Softmax DARTS (PipeSoftmax) and Pipelined Gumbel-softmax DARTS (PipeGumbel) systems.

### 2.4. Penalized DARTS

In order to flexibly adjust the trade-off between system performance and complexity, a penalized loss function incorporating the underlined neural network size is used.

$$\mathcal{L} = \mathcal{L}_{LF-MMI} + \eta \sum_{l,i} \lambda_i^l C_i^l, \quad (6)$$

where  $C_i^l$  is the number of parameters of the  $i$ -th candidate considered at the  $l$ -th layer, and  $\eta$  is the penalty scaling factor empirically set for different tasks.

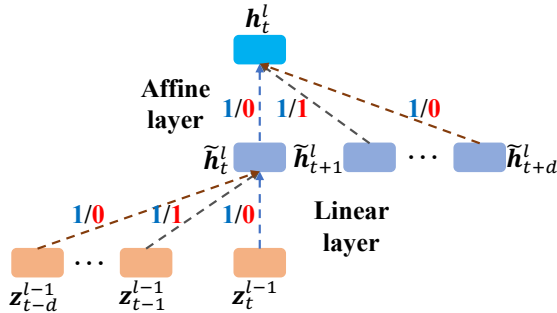


Figure 2: Example part of a supernet containing all the context offsets for a TDNN-F layer. Dashed lines with different colors represent different context choices in each linear (left context) and affine (right context) transforms. The blue integers denote the supernet system using all the context offsets, while the red integers represent a candidate offset choice of  $\pm 1$ .

## 2.5. NAS lattice

When the architecture weights are learned using various NAS methods presented in Sec. 2, all the candidate architectures contained in the supernet can be represented by a NAS lattice carrying their associated weights. An example part of a NAS lattice for determining the TDNN-F left and right context offsets is shown in Fig. 1.

## 3. Search Space and Parameter Sharing

This section describes the search space and its implementation when NAS methods of Sec. 2 are used to automatically learn two hyper-parameters of TDNN-F models: i) the left and right splicing context offsets; and ii) the dimensionality of the bottleneck linear projection at each hidden layer. Parameter sharing among candidate architectures used to facilitate efficient search over a large number of TDNN-F systems is also presented.

### 3.1. TDNN-F Context Offset Search Space

Context offset settings play an important role in modeling the long temporal information in TDNN-F models. However, manually selecting context offsets is time-consuming for different applications. Inspired by the parameter-sharing used in earlier NAS research [10], we design a TDNN-F supernet (Fig. 2) to contain all possible choices of context offsets to the left ( $\{-d, 0\}$ ,  $\dots$ ,  $\{-1, 0\}$ ,  $\{0, 0\}$ ) and right ( $\{0, 0\}$ ,  $\{0, 1\}$ ,  $\dots$ ,  $\{0, d\}$ ) at each layer during search. Note that  $0, d$  denote context offsets of 0 and  $d$  (right). For the supernet system, it requires the sparse context connection weights to be densely set as 1 for all context offsets. Any candidate TDNN-F model with particular context offsets, out of the total  $(d + 1)^{2L}$  possible choices, contained in the supernet is represented by setting the corresponding connection weights to be 1, while setting the others to be 0.

### 3.2. TDNN-F Bottleneck Dimensionality Search Space

Similarly, a TDNN-F supernet containing all the candidate TDNN-F with different projection dimensions is designed, as shown in Fig. 3 for one hidden layer. When applying the NAS methods in Sec. 2,  $\phi_i^l(\cdot)$  of Eq. 1 is set as an identity matrix. In common with the standard TDNN-F model, the weight matrix  $\mathbf{W}_i^l$  of  $i$ -th architecture choice in  $l$ -th layer is factored into one semi-orthogonal weight matrix  $\widetilde{\mathbf{W}}_{0:n_i-1}^l$  and one affine weight matrix  $\widehat{\mathbf{W}}_{0:n_i-1}^l$  as shown in Fig. 3.  $n_i$  is the dimensionality of the  $i$ -th architecture. Parameter sharing among differ-

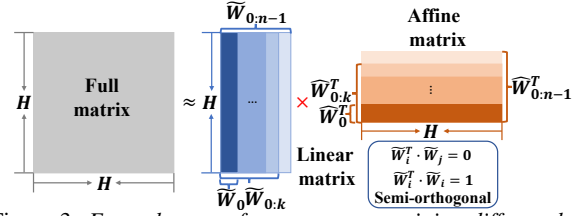


Figure 3: Example part of a supernet containing different bottleneck projection dimensionality choices in the TDNN-F hidden layer. The full weight matrix is factored into one semi-orthogonal linear supernet weight matrix  $\widetilde{\mathbf{W}}_{0:n-1}^l$  and one affine supernet weight matrix  $\widehat{\mathbf{W}}_{0:n-1}^l$ . Architectures with different projection dimensions are represented by the corresponding submatrices starting from the first column.

ent candidate architectures' linear matrices  $\widetilde{\mathbf{W}}_{0:k}$  (left and right from the first column) and affine matrices  $\widehat{\mathbf{W}}_{0:k}$  (left and right from the first column) ( $0 \leq k \leq n - 1$ ) is implemented by the corresponding submatrices extracted from the largest matrix  $\widetilde{\mathbf{W}}_{0:n-1}^l$ . Such sharing allows a large number of TDNN-F projection dimensionality choices at each layer, e.g., selected from 25, 50, 80, 100, 120, 160, 200, 240 as considered in this paper, to be compared for selection during search. This leads to a total of  $8^{14}$  candidate TDNN-F systems to be selected from.

## 4. Experimental Results

This section presents our experiments carried out on the 300-hour Switchboard telephone speech recognition tasks using Kaldi toolkit [31]. The GMM-HMM system [32, 33], TDNN-F acoustic model [4], and language model are similar to those described in [34]. The TDNN-F baseline system is configured with the default setting in Kaldi script<sup>1</sup>, except that we use 40-dimension filterbank features as the input features. In the searching stage, TDNN-F supernet models are trained on the training set with one thread for 3 epochs, while architecture parameters of PipeSoftmax and PipeGumbel systems are updated for additional 3 epochs using a held-out data set by fixing the normal DNN parameters. Note that we randomly select 5% of the original training set as the held-out data set and  $T$  in Gumbel-Softmax distribution is annealed from 1 to 0.03 in our experiments. Once candidate TDNN-F models are derived from the searching stage, they are trained for 3 epochs from scratch.

### 4.1. TDNN-F Context Offset Search Results

In this section, we describe the experimental results of searching context offsets at each layer by using various NAS methods introduced in Sec. 2, as shown in Table 1. Systems (5)-(8), (13)-(14) perform the search over the total  $4^{28}$  TDNN-F choices with maximum context offsets of  $\pm 3$ , while systems (9)-(12) perform the search over  $7^{28}$  TDNN-F choices with the maximum context offsets of  $\pm 6$ . Systems (5), (7), (9), (11), (13), (14) are the top 1 systems extracted from the NAS lattices. The top 5 (Sys (6), (8), (10), (12)) selected and their associated word error rate (WER) means and standard deviations are also shown in Table 1. There are several trends observed from the results in Table 1. First, the Gumbel-Softmax DARTS system (Sys (11)) outperforms the baseline Kaldi recipe<sup>1</sup> TDNN-F system (Sys (1)) by **0.3%** and **1.0%** absolute WER reductions on the SWBD and CallHome test sets. Even compared with additional manually designed TDNN-F systems (Sys (3)), the Gumbel-Softmax

<sup>1</sup>Based on the published Kaldi code at [github.com/kaldi-asr/kaldi/egs/swbd/s5c/local/chain/run\\_tdnn.sh](https://github.com/kaldi-asr/kaldi/egs/swbd/s5c/local/chain/run_tdnn.sh)

DARTS system (Sys 11) still produces **0.3%** absolute WER reduction on the CallHome test set. Second, Gumbel-Softmax DARTS systems (Sys (7), (11)) obtain both better performance and more accurate model ranking than Softmax DARTS systems (Sys (5), (9)), which can be verified from the WER means of top 5 (Sys (6), (8), (10), (12)).

Table 1: *Performance (WER%) comparison of TDNN-F models (#param:18M) configured with context offsets produced by the baseline system, manual designed systems, Softmax DARTS (Softmax), Gumbel-Softmax DARTS (Gumbel), Pipelined Softmax DARTS (PipeSoftmax), Pipelined Gumbel-Softmax DARTS (PipeGumbel) systems described in Sec. 2.  $\{[a, b]\}: \{-c, d\}$  denotes context offsets  $\{-c, 0\}$  to the left and  $\{0, d\}$  to the right used from a-th layer to b-th layer inclusive.*

| Sys  | Method                   | Context Offsets   | Hub5' 00        |                 |  |  |  |  |          |  |  |  |  |  | #param |
|------|--------------------------|---|-----------------|-----------------|--|--|--|--|----------|--|--|--|--|--|--------|
|      |                          |   | SWBD            |                 |  |  |  |  | CallHome |  |  |  |  |  |        |
| (1)  | Baseline <sup>[31]</sup> | $\{[1,3]\}: \{-1,1\}; \{4\}: \{0\}; \{[5,14]\}: \{-3,3\}$   | 10.0            | 20.8            |  |  |  |  |          |  |  |  |  |  | 18M    |
| (2)  |                          | $\{[1,3]\}: \{-1,1\}; \{4\}: \{0\}; \{[5,14]\}: \{-6,6\}$   | <b>9.8</b>      | <b>20.1</b>     |  |  |  |  |          |  |  |  |  |  |        |
| (3)  | Manual                   | $\{[1,3]\}: \{-1,1\}; \{4\}: \{0\}; \{[5,14]\}: \{-9,9\}$   | <b>9.7</b>      | <b>20.1</b>     |  |  |  |  |          |  |  |  |  |  |        |
| (4)  |                          | $\{[1,3]\}: \{-1,1\}; \{4\}: \{0\}; \{[5,14]\}: \{-12,12\}$   | 10.1            | 20.8            |  |  |  |  |          |  |  |  |  |  |        |
| (5)  | Softmax top1             | $\{1\}: \{0,1\}; \{[2,14]\}: \{-3,3\}$  | 10.2            | 20.6            |  |  |  |  |          |  |  |  |  |  |        |
| (6)  | Top5                     | Maximum context offsets $\pm 3$   | $10.0 \pm 0.13$ | $20.6 \pm 0.13$ |  |  |  |  |          |  |  |  |  |  |        |
| (7)  | Gumbel top1              | $\{[1,2]\}: \{-2,2\}; \{[3,4]\}: \{-2,3\}; \{[5,14]\}: \{-3,3\}$  | 9.9             | 20.1            |  |  |  |  |          |  |  |  |  |  |        |
| (8)  | Top5                     | Maximum context offsets $\pm 3$   | $10.0 \pm 0.08$ | $20.3 \pm 0.13$ |  |  |  |  |          |  |  |  |  |  |        |
| (9)  | Softmax top1             | $\{1\}: \{0,1\}; \{2\}: \{-6,1\}; \{3\}: \{-6,2\}; \{[4,14]\}: \{-6,6\}$  | 9.7             | 20.1            |  |  |  |  |          |  |  |  |  |  |        |
| (10) | Top5                     | Maximum context offsets $\pm 6$   | $9.7 \pm 0.14$  | $20.2 \pm 0.13$ |  |  |  |  |          |  |  |  |  |  |        |
| (11) | Gumbel top1              | $\{[1,2]\}: \{-3,2\}; \{3\}: \{-4,3\}; \{[4,5]\}: \{-4,4\}; \{[6,7]\}: \{-4,6\}; \{8\}: \{-5,6\}; \{[9,14]\}: \{-6,6\}$ | <b>9.7</b>      | <b>19.8</b>     |  |  |  |  |          |  |  |  |  |  |        |
| (12) | Top5                     | Maximum context offsets $\pm 6$   | $9.7 \pm 0.17$  | $20.0 \pm 0.19$ |  |  |  |  |          |  |  |  |  |  |        |
| (13) | PipeSoftmax top1         | $\{1\}: \{-1,3\}; \{[2,4,12,14]\}: \{-3,3\}; \{3\}: \{-2,3\}; \{[13]\}: \{0,3\}$  | 9.9             | 20.4            |  |  |  |  |          |  |  |  |  |  |        |
| (14) | PipeGumbel top1          | $\{1\}: \{-1,3\}; \{2,3\}: \{-2,3\}; \{4\}: \{-3,2\}; \{[5,6,14]\}: \{-3,3\}; \{7\}: \{0,3\}$                           | 9.9             | 20.4            |  |  |  |  |          |  |  |  |  |  |        |

## 4.2. TDNN-F Bottleneck Dimensionality Search

Table 2 shows the performance of searching bottleneck projection dimensions at each layer using NAS methods over the following choices: 25,50,80,100,120,160,200,240. This leads to a total of  $8^{14}$  TDNN-F systems to be selected from. Systems (9)-(14) are the top 1 systems extracted from the NAS lattices. In comparison with the baseline Kaldi recipe [31] TDNN-F system (Sys (1)), the Pipelined DARTS<sup>2</sup> systems (Sys (11), (12)) with the same number of parameters achieve comparable performance. If we further add the resource penalty to the objective loss function, the PipeGumbel system (Sys (14)) can produce **0.4%** absolute WER reduction on the CallHome test set and a relative model size reduction of **20%** over the baseline Kaldi recipe [31] TDNN-F system (Sys (1)), by selecting fewer bottleneck projection dimensions at higher layers. In addition, the Softmax DARTS system (Sys 9) does not outperform the baseline Kaldi recipe TDNN-F system (Sys (1)), which may be explained as prematurely selecting sub-optimal structures at an early stage when both architecture weights and normal DNN parameters are being trained before reaching convergence.

## 4.3. Search of both Context Offsets & Projection Dims

The performance of searching both context offsets and bottleneck projection dimensionality by NAS methods is shown in Table 3. Based on the context offsets determined using "Gumbel Top1" (Sys (11) in Table 1), the PipeGumbel method is used to further select the projection dimensions. This leads to the system (2) in table 3, which produces **0.3%/0.6%** absolute WER reductions on the SWBD/CallHome test sets and a relative model size reduction of **29.4%** over the baseline Kaldi recipe TDNN-F system (Sys (1) in Table 1). In a reversed order, by performing the search of the bottleneck projection di-

<sup>2</sup>Updating the architecture weights of Pipelined DARTS systems on the training data produces worse results than that using held-out data.

Table 2: *Performance (WER%) comparison of TDNN-F models configured with varying bottleneck projection dimensions produced by the baseline system, manual designed systems, Softmax DARTS (Softmax), Gumbel-Softmax DARTS (Gumbel), Pipelined Softmax DARTS (PipeSoftmax), Pipelined Gumbel-Softmax DARTS (PipeGumbel) systems in Sec. 2.  $\eta$  is the penalty scaling factor in Eqn. (6).*

| Sys  | Method                           | Bottleneck Projection Dimensionality (1-th to 14-th layer)  | Hub5' 00   |             |              |  |  |  |          |  |  |  |  |  | #param |
|------|----------------------------------|---|------------|-------------|--------------|--|--|--|----------|--|--|--|--|--|--------|
|      |                                  |   | SWBD       |             |              |  |  |  | CallHome |  |  |  |  |  |        |
| (1)  | Baseline <sup>[31]</sup>         | 160 160 160 160 160 160 160 160 160 160 160 160 160 160 160 | 10.0       | 20.8        |              |  |  |  |          |  |  |  |  |  | 18M    |
| (2)  |                                  | 25 25 25 25 25 25 25 25 25 25 25 25 25 25 25                | 11.2       | 23.5        | 7M           |  |  |  |          |  |  |  |  |  |        |
| (3)  |                                  | 50 50 50 50 50 50 50 50 50 50 50 50 50 50                   | 10.3       | 21.6        | 9M           |  |  |  |          |  |  |  |  |  |        |
| (4)  | Manual                           | 80 80 80 80 80 80 80 80 80 80 80 80 80 80                   | 10.2       | 21.1        | 11M          |  |  |  |          |  |  |  |  |  |        |
| (5)  |                                  | 100 100 100 100 100 100 100 100 100 100 100 100 100 100     | 10.0       | 20.6        | 13M          |  |  |  |          |  |  |  |  |  |        |
| (6)  |                                  | 120 120 120 120 120 120 120 120 120 120 120 120 120 120     | 10.0       | 20.7        | 15M          |  |  |  |          |  |  |  |  |  |        |
| (7)  |                                  | 200 200 200 200 200 200 200 200 200 200 200 200 200 200     | 10.2       | 20.1        | 21M          |  |  |  |          |  |  |  |  |  |        |
| (8)  |                                  | 240 240 240 240 240 240 240 240 240 240 240 240 240 240     | 10.1       | 20.5        | 24M          |  |  |  |          |  |  |  |  |  |        |
| (9)  | Softmax top1                     | 25 25 25 25 25 240 240 240 240 240 240 240 240 240          | 10.2       | 21.3        | 17M          |  |  |  |          |  |  |  |  |  |        |
| (10) | Gumbel top1                      | 100 100 120 25 160 160 200 200 160 200 160 160 160 160      | 10.1       | 20.5        | 17M          |  |  |  |          |  |  |  |  |  |        |
| (11) | PipeSoftmax top1                 | 240 200 200 120 240 200 120 200 200 200 200 200 200 200     | 10.2       | 20.5        | 17M          |  |  |  |          |  |  |  |  |  |        |
| (12) | PipeGumbel top1                  | 200 200 200 120 240 200 120 200 200 200 200 200 200 200     | 9.9        | 20.7        | 18M          |  |  |  |          |  |  |  |  |  |        |
| (13) | PipeSoftmax top1 ( $\eta=0.02$ ) | 160 100 120 25 200 160 160 160 160 160 160 160 160 160      | 10.2       | 21.0        | 14.1M        |  |  |  |          |  |  |  |  |  |        |
| (14) | PipeGumbel top1 ( $\eta=0.03$ )  | 160 100 120 25 120 160 120 100 120 100 50 80 200 200        | <b>9.9</b> | <b>20.4</b> | <b>14.6M</b> |  |  |  |          |  |  |  |  |  |        |

mensionality (Sys (14) in Table 2) first and then searching the context offsets using the Gumbel-Softmax DARTS method, the system (3) in table 3 produces a comparable performance in comparison with the system (1). By searching the context offsets (first stage of PipeGumbel) and projection dimensions in the same supernet, the best performance is achieved by the system (4), which produces **0.4%/1.0%** absolute WER reductions on the SWBD/CallHome test sets and a relative model size reduction of **28%** over the baseline Kaldi recipe TDNN-F system.

Table 3: *Performance (WER%) comparison of TDNN-F models configured with both context offsets and projection dimensions produced by Gumbel-Softmax DARTS (Gumbel), Pipelined Gumbel-Softmax DARTS (PipeGumbel) systems. "→" denotes the searching order of context offsets and dimensions. "+" denotes offsets and dimensions are searched in the same supernet.*

| Sys | Method   | Bottleneck Projection Dimensionality/Context Offsets  | $\eta$ | Hub5' 00   |             |              |  |  |  |          |  |  |  |  |  | #param |
|-----|--|---|--------|------------|-------------|--------------|--|--|--|----------|--|--|--|--|--|--------|
|     |  |   |        | SWBD       |             |              |  |  |  | CallHome |  |  |  |  |  |        |
| (1) | context  | 100 160 160 100 120 100 100 100 120 80 120 25 160 240   | 0.05   | 9.7        | 19.9        | 14.8M        |  |  |  |          |  |  |  |  |  |        |
|     | (Gumbel top1, Sys (14), Table 1)                   | $\{1,2\}: \{-3,2\}; \{3\}: \{-4,3\}; \{4,5\}: \{-4,4\}; \{6,7\}: \{-4,6\}; \{8\}: \{-5,6\}; \{[9,14]\}: \{-6,6\}$                                 |        |            |             |              |  |  |  |          |  |  |  |  |  |        |
| (2) | → dim  | 100 100 100 100 100 80 80 100 100 100 80 100 25 120 160   | 0.1    | <b>9.7</b> | <b>20.2</b> | <b>12.7M</b> |  |  |  |          |  |  |  |  |  |        |
|     | (PipeGumbel top1)                                  | $\{1,2\}: \{-3,2\}; \{3\}: \{-4,3\}; \{4,5\}: \{-4,4\}; \{6,7\}: \{-4,6\}; \{8\}: \{-5,6\}; \{[9,14]\}: \{-6,6\}$                                 |        |            |             |              |  |  |  |          |  |  |  |  |  |        |
| (3) | dim (PipeGumbel top1, Sys (14), Table 2) → context | 160 100 120 25 120 160 120 100 120 100 50 80 200 200  | 0.03   | 10.0       | 19.7        | 14.6M        |  |  |  |          |  |  |  |  |  |        |
|     | (Gumbel top1)                                      | $\{1,4\}: \{-2,2\}; \{2\}: \{-2,4\}; \{3,4\}: \{-3,3\}; \{5\}: \{-3,2\}; \{6\}: \{-3,4\}; \{7\}: \{-4,4\}; \{8\}: \{-4,6\}; \{[9,14]\}: \{-6,6\}$ |        |            |             |              |  |  |  |          |  |  |  |  |  |        |
| (4) | dim (PipeGumbel top1)                              | 160 100 100 120 100 80 80 120 50 80 80 100 120  | 0.03   | <b>9.6</b> | <b>19.8</b> | <b>13.0M</b> |  |  |  |          |  |  |  |  |  |        |
|     | (Gumbel top1)                                      | $\{1\}: \{-2,2\}; \{2\}: \{-2,4\}; \{3,4\}: \{-3,3\}; \{5\}: \{-3,2\}; \{6\}: \{-3,4\}; \{7\}: \{-4,4\}; \{8\}: \{-4,6\}; \{[9,14]\}: \{-6,6\}$   |        |            |             |              |  |  |  |          |  |  |  |  |  |        |

## 5. Conclusions

In this paper, a range of neural architecture search (NAS) techniques are investigated to automatically learn two hyperparameters that heavily affect the performance and model complexity of state-of-the-art factored time delay neural network (TDNN-F) acoustic models: i) the left and right splicing context offsets; and ii) the dimensionality of the bottleneck linear projection at each hidden layer. Experimental results suggest NAS techniques can be used for the automatic configuration of DNN based speech recognition systems and allow their wider application to different tasks.

## 6. Acknowledgements

This research is supported by Hong Kong Research Grants Council General Research Fund No.14200218, Theme Based Research Scheme T45-407/19N and Shun Hing Institute of Advanced Engineering Project No.MMT-p1-19.

## 7. References

- [1] B. Kingsbury, "Lattice-based optimization of sequence classification criteria for neural-network acoustic modeling," in *2009 IEEE International Conference on Acoustics, Speech and Signal Processing*. IEEE, 2009, pp. 3761–3764.
- [2] K. Vesely, A. Ghoshal, L. Burget, and D. Povey, "Sequence-discriminative training of deep neural networks," in *Interspeech*, vol. 2013, 2013, pp. 2345–2349.
- [3] H. Su, G. Li, D. Yu, and F. Seide, "Error back propagation for sequence training of context-dependent deep networks for conversational speech transcription," in *2013 IEEE International Conference on Acoustics, Speech and Signal Processing*. IEEE, 2013, pp. 6664–6668.
- [4] D. Povey, V. Pediinti, D. Galvez, P. Ghahremani, V. Manohar, X. Na, Y. Wang, and S. Khudanpur, "Purely sequence-trained neural networks for asr based on lattice-free mmi," in *Interspeech*, 2016, pp. 2751–2755.
- [5] T. Elsken, J. H. Metzen, and F. Hutter, "Neural architecture search: A survey," *arXiv preprint arXiv:1808.05377*, 2018.
- [6] K. O. Stanley and R. Miikkulainen, "Evolving neural networks through augmenting topologies," *Evolutionary computation*, vol. 10, no. 2, pp. 99–127, 2002.
- [7] K. Kandasamy, W. Neiswanger, J. Schneider, B. Poczos, and E. P. Xing, "Neural architecture search with bayesian optimisation and optimal transport," in *Advances in Neural Information Processing Systems*, 2018, pp. 2016–2025.
- [8] B. Zoph and Q. V. Le, "Neural architecture search with reinforcement learning," *arXiv preprint arXiv:1611.01578*, 2016.
- [9] B. Baker, O. Gupta, N. Naik, and R. Raskar, "Designing neural network architectures using reinforcement learning," *arXiv preprint arXiv:1611.02167*, 2016.
- [10] H. Pham, M. Y. Guan, B. Zoph, Q. V. Le, and J. Dean, "Efficient neural architecture search via parameter sharing," *arXiv preprint arXiv:1802.03268*, 2018.
- [11] H. Cai, T. Chen, W. Zhang, Y. Yu, and J. Wang, "Efficient architecture search by network transformation," in *Thirty-Second AAAI conference on artificial intelligence*, 2018.
- [12] Z. Zhong, J. Yan, W. Wu, J. Shao, and C.-L. Liu, "Practical block-wise neural network architecture generation," in *Proceedings of the IEEE conference on computer vision and pattern recognition*, 2018, pp. 2423–2432.
- [13] H. Liu, K. Simonyan, and Y. Yang, "Darts: Differentiable architecture search," *arXiv preprint arXiv:1806.09055*, 2018.
- [14] S. Xie, H. Zheng, C. Liu, and L. Lin, "Snas: stochastic neural architecture search," *arXiv preprint arXiv:1812.09926*, 2018.
- [15] H. Cai, L. Zhu, and S. Han, "Proxylessnas: Direct neural architecture search on target task and hardware," *arXiv preprint arXiv:1812.00332*, 2018.
- [16] F. P. Casale, J. Gordon, and N. Fusi, "Probabilistic neural architecture search," *arXiv preprint arXiv:1902.05116*, 2019.
- [17] S. Hu, S. Xie, H. Zheng, C. Liu, J. Shi, X. Liu, and D. Lin, "Dsnas: Direct neural architecture search without parameter retraining," in *The IEEE Conference on Computer Vision and Pattern Recognition (CVPR)*, June 2020.
- [18] A. Waibel, "Consonant recognition by modular construction of large phonemic time-delay neural networks," in *Advances in neural information processing systems*, 1989, pp. 215–223.
- [19] V. Pediinti, D. Povey, and S. Khudanpur, "A time delay neural network architecture for efficient modeling of long temporal contexts," in *Sixteenth Annual Conference of the International Speech Communication Association*, 2015.
- [20] D. Povey, G. Cheng, Y. Wang, K. Li, H. Xu, M. Yarmohammadi, and S. Khudanpur, "Semi-orthogonal low-rank matrix factorization for deep neural networks," in *Interspeech*, 2018, pp. 3743–3747.
- [21] E. Real, A. Aggarwal, Y. Huang, and Q. V. Le, "Regularized evolution for image classifier architecture search," in *Proceedings of the aaai conference on artificial intelligence*, vol. 33, 2019, pp. 4780–4789.
- [22] M. Tan and Q. V. Le, "Mixconv: Mixed depthwise convolutional kernels," *CoRR, abs/1907.09595*, 2019.
- [23] C. Liu, L.-C. Chen, F. Schroff, H. Adam, W. Hua, A. L. Yuille, and L. Fei-Fei, "Auto-deeplab: Hierarchical neural architecture search for semantic image segmentation," in *The IEEE Conference on Computer Vision and Pattern Recognition (CVPR)*, June 2019.
- [24] P. Lin, P. Sun, G. Cheng, S. Xie, X. Li, and J. Shi, "Graph-guided architecture search for real-time semantic segmentation," *arXiv preprint arXiv:1909.06793*, 2019.
- [25] V. Nekrasov, H. Chen, C. Shen, and I. Reid, "Fast neural architecture search of compact semantic segmentation models via auxiliary cells," in *The IEEE Conference on Computer Vision and Pattern Recognition (CVPR)*, June 2019.
- [26] Y. Chen, T. Yang, X. Zhang, G. Meng, C. Pan, and J. Sun, "Detnas: Neural architecture search on object detection," *arXiv preprint arXiv:1903.10979*, 2019.
- [27] T. Véniat, O. Schwander, and L. Denoyer, "Stochastic adaptive neural architecture search for keyword spotting," in *ICASSP 2019-2019 IEEE International Conference on Acoustics, Speech and Signal Processing (ICASSP)*. IEEE, 2019, pp. 2842–2846.
- [28] H. Mazzawi, X. Gonzalvo, A. Kracun, P. Sridhar, N. Subrahmanyam, I. L. Moreno, H. J. Park, and P. Violette, "Improving keyword spotting and language identification via neural architecture search at scale," *Proc. Interspeech 2019*, pp. 1278–1282, 2019.
- [29] C. J. Maddison, A. Mnih, and Y. W. Teh, "The concrete distribution: A continuous relaxation of discrete random variables," *arXiv preprint arXiv:1611.00712*, 2016.
- [30] Z. Guo, X. Zhang, H. Mu, W. Heng, Z. Liu, Y. Wei, and J. Sun, "Single path one-shot neural architecture search with uniform sampling," *arXiv preprint arXiv:1904.00420*, 2019.
- [31] D. Povey, A. Ghoshal, G. Boulianne, and et al., "The kaldi speech recognition toolkit," *Tech. Rep.*, 2011.
- [32] C. J. Leggetter and P. C. Woodland, "Maximum likelihood linear regression for speaker adaptation of continuous density hidden markov models," *Computer speech & language*, vol. 9, no. 2, pp. 171–185, 1995.
- [33] M. J. Gales, "Maximum likelihood linear transformations for hmm-based speech recognition," *Computer speech & language*, vol. 12, no. 2, pp. 75–98, 1998.
- [34] S. Hu, X. Xie, S. Liu, M. W. Lam, J. Yu, X. Wu, X. Liu, and H. Meng, "Lf-mmi training of bayesian and gaussian process time delay neural networks for speech recognition," *Proc. Interspeech 2019*, pp. 2793–2797, 2019.